HHS Public Access

Author manuscript

Neurobiol Aging. Author manuscript; available in PMC 2017 August 30.

Published in final edited form as:

Neurobiol Aging. 2015 July ; 36(7): 2319–2330. doi:10.1016/j.neurobiolaging.2015.04.004.

Partial loss of the DNA repair scaffolding protein, *Xrcc1*, results in increased brain damage and reduced recovery from ischemic stroke in mice

Somnath Ghosh[1], **Chandrika Canugovi**[1], **Jeong Seon Yoon**[2], **David M. Wilson III**[1], **Deborah L. Croteau**[1], **Mark P. Mattson**[2], and **Vilhelm A. Bohr**[1,*]

[1]Laboratory of Molecular Gerontology, National Institute on Aging, Intramural Research Program (NIA IRP). Biomedical Research Center, 251 Bayview Blvd., Baltimore, MD 21224

[2]Laboratory of Neurosciences, National Institute on Aging, Intramural Research Program (NIA IRP). Biomedical Research Center, 251 Bayview Blvd., Baltimore, MD 21224

Abstract

Oxidative DNA damage is mainly repaired by base excision repair (BER). Previously, our lab showed that mice lacking the BER glycosylases Ogg1 or Neil1 recover more poorly from focal ischemic stroke than wild-type mice. Here, a mouse model was used to investigate whether loss of one of the two alleles of *Xrcc1*, which encodes a non-enzymatic scaffold protein required for BER, alters recovery from stroke. Ischemia and reperfusion caused higher brain damage and lower functional recovery in $Xrcc1^{+/-}$ mice than in wild-type mice. Additionally, a greater percentage of $Xrcc1^{+/-}$ mice died as a result of the stroke. Brain samples from human individuals who died of stroke and individuals who died of non-neurological causes were assayed for various steps of BER. Significant losses of thymine glycol incision, abasic endonuclease incision and single nucleotide incorporation activities were identified, as well as lower expression of XRCC1 and NEIL1 proteins in stroke brains compared to controls. Together, these results suggest that impaired BER is a risk factor in ischemic brain injury and contributes to its recovery.

Keywords

Base excision repair; Stroke; Xrcc1; Oxidative stress

1. Introduction

Neurons encounter periods of oxidative stress because of their high metabolic requirements needed to support electrical and synaptic activities. During ischemic stroke, excessive

*Corresponding author at: Laboratory of Molecular Gerontology, National Institute on Aging, 251 Bayview Blvd, Baltimore, MD 21224, USA. Tel.: + 1 410 558 8162; fax: +1 410 558 8157. vbohr@nih.gov.

Disclosure statement

Authors have no conflicts of interest

oxidative stress is generated increasing the burden on stress resistance mechanisms, including the repair of oxidatively damaged DNA. Thus, the integrity of repair systems that restore damaged DNA is critical for the survival and normal function of neurons. Oxidative DNA damage mainly includes modified bases, abasic sites and single strand breaks. The major pathway responsible for the repair of these forms of DNA damage is BER, and its related sub-pathway, single strand break repair (SSBR) (Canugovi, et al., 2013).

Enzymes in the BER pathway coordinately recognize and remove oxidative DNA lesions, such as 8-oxoguanine (8-oxo-dG). The first step of BER is mediated by a DNA glycosylase, such as 8-oxo-dG glycosylase 1 (OGG1), which releases the damaged base from the DNA backbone by cleaving the glycosidic bond. In the next step of BER, the phosphodiester bond in the DNA backbone is cleaved by an apurinic/apyrimidinic (AP) endonuclease, after which the DNA ends are processed. The missing nucleotide(s) are replaced by a gap-filling DNA polymerase, and the nicked DNA is sealed by a DNA ligase (Tomkinson, et al., 2006).

X-ray repair cross-complementing protein 1 (XRCC1) is a non-enzymatic scaffold protein that interacts with several BER enzymes, including DNA glycosylases (Campalans, et al., 2005,Marsin, et al., 2003), human AP endonuclease 1 (APE1) (Vidal, et al., 2001), DNA polymerase β (POLβ) (Caldecott, et al., 1996,Marintchev, et al., 2000), and DNA ligase IIIα (Mani, et al., 2007,Mortusewicz and Leonhardt, 2007). XRCC1 stimulates the activity of DNA glycosylases that repair oxidative and alkylated base lesions and stimulates the AP endonuclease and 3′-phosphodiesterase activities of APE1. XRCC1 also binds to and enhances DNA damage-specific binding of polynucleotide kinase/phosphatase (PNKP) (Mani, et al., 2007), accelerating repair of DNA SSBs (Whitehouse, et al., 2001). Furthermore, DNA ligase IIIα (LIG3α) is stabilized through a specific interaction between its C-terminal BRCT domain and the BRCT II domain of XRCC1 (Taylor, et al., 1998). XRCC1 also interacts with tyrosyl-DNA phosphodiesterase 1 (TDP1) and Aprataxin (APTX), which excise 3’ or 5’ end blocking groups from DNA, such as 3’-phosphate, 3’-tyrosyl and 5’-AMP residues (Caldecott, 2008,Wilson and Mattson, 2007). Mutations in *TDP1* or *APTX* are linked to the neurodegenerative disorders spinocerebellar ataxia with axonal neuropathy (SCAN1) and ataxia-oculomotor apraxia 1 (AOA1), respectively (Date, et al., 2001,Moreira, et al., 2001,Takashima, et al., 2002). During direct SSBR, poly(ADP–ribose) polymerase (PARP) likely recognizes the single strand break and recruits XRCC1, which in-turn coordinates PNKP, POLβ and LIG3α to complete the repair process. Thus, biochemical and genetic studies suggest that XRCC1 plays crucial roles in BER/SSBR with potentially important roles in protecting neuronal cells against oxidative stress (Kulkarni, et al., 2008) and promoting neurogenesis during development (Lee, et al., 2009).

In mice, deletion of both alleles of *Xrcc1* leads to early embryonic lethality (Tebbs, et al., 1999). In a comprehensive study, Xrcc1 heterozygous ($Xrcc1^{+/-}$) mice did not show any signs of accelerated aging (McNeill, et al., 2011). Further, the brain histology and behavior were normal, but curiously, some $Xrcc1^{+/-}$ mice showed organ rupture. While motor coordination and overall activity were deemed normal in the $Xrcc1^{+/-}$ mice, it is noteworthy that a small number of animals exhibited behavioral features commonly associated with stroke, namely impaired lower leg movement or tilting of the head (McNeill, et al., 2011).

Stroke is a neurological disease that causes brain damage and injury due to acute oxidative stress, and is the second leading cause of neurological disability following dementia (http://www.world-heart-federation.org/cardiovascular-health/stroke/). While limiting the acute effects of stroke is of very high importance, the speedy recovery after stroke is just as important. A slow recovery is associated with long term neurological sequelae and is very costly for the individual and the society. Thus investigation of how the recovery after stroke can be improved is as important as identification of risk factors for stroke. The role of BER in antagonizing acute oxidative stress may be significant in stroke survivors. Therefore, understanding the role of BER and its components in response to stroke in human tissue and animal models is an important line of investigation. We previously showed that mice lacking either Ogg1 or Neil1, glycosylases that initiate BER of oxidative base lesions, recovered more poorly from stroke than the wild type (Canugovi, et al., 2012,Liu, et al., 2011). We here examine whether mice haploinsufficient for the BER/SSBR protein, XRCC1, are more affected by stroke induction.

Our results indicate that partial loss of the DNA repair protein, Xrcc1 renders brain cells vulnerable to oxidative stress after ischemic injury. We have also examined the relative activity levels of BER components in human stroke affected post-mortem and age-matched control brains. We find that, individual who died of stroke had a significant impairment in BER function. Together, our results underscore the importance of BER and further argue that BER genotypes should be evaluated as a risk factor for stroke and its recovery

2. Materials and methods

2.1. Mice

Xrcc1$^{+/-}$ and littermate wild-type mice (McNeill, et al., 2011) were used for all experiments. Five to twelve month-old male mice were used for the experiments. Mice were maintained in a constant-temperature facility with a 12 h light/12 h dark cycle, and free access to food and water. All procedures were approved by the Animal Care and Use Committee of the National Institute on Aging Intramural Research Program.

2.2. Rotarod

This test was used to analyze the motor function and endurance in mice. The rotarod machine (Med Associates) has nine different fixed speeds and an accelerating speed program. The parameters tested and recorded in each case were the number of falls in 5 min duration and the latency to the first fall. All mice were trained and tested for their motor ability at 2–20 rpm before middle cerebral artery occlusion/reperfusion (MCAO/R) procedure. After MCAO/R, the accelerating rotarod test was performed at the 24 h and 48 h time points.

2.3. Middle Cerebral Artery Occlusion and Reperfusion

The focal ischemia/reperfusion model was performed using the intraluminal suture technique described previously; the left middle cerebral artery was occluded for 1 h (Arumugam, et al., 2010). Body temperature was maintained at 37 °C using heating pads and a heatin g lamp throughout the surgical procedure and afterward until the mouse

recovered from anesthesia. In a separate set of experiments anesthetized animals from all groups (three mice per group) underwent cerebral blood flow (CBF) measurements using a laser Doppler perfusion monitor. All CBF measurements were performed with the mouse fixed in a plastic frame with the probe placed in the region of cerebral cortex perfused by the middle cerebral artery (MCA).

2.4. Evaluation of Neurological Deficits and Infarct Volume

Neurological impairment was assessed using a five-point neurological deficit score (0, no neurological deficit; 1, failure to extend left paw; 2, circling to the left; 3, falling to the left; and 4, unable to walk spontaneously) (Bederson, et al., 1986) and were assessed without knowledge of mouse genotype. Differences between groups were analyzed by a nonparametric Kruskal–Wallis one-way ANOVA test at 5% significance level. At 48 h after the experimental stroke, the mice were euthanized and infarct area was evaluated by 2,3,5-triphenyltetrazolium chloride (TTC) staining as described previously (Arumugam, et al., 2010). For each brain section, the infarct area was determined by subtracting the area of the non-infarcted ipsilateral hemisphere from that of the intact contralateral hemisphere. The percentage of infarct volume was calculated by dividing the sum of the area from all sections of infarction by the total of that of contralateral hemisphere to avoid the influence of tissue edema (Swanson and Sharp, 1994). A nonparametric statistical test (Mann–Whitney test) and also a two-sample t-test were conducted to analyze the significance of the data.

2.5. Immunoblot analysis

Mice were euthanized by cervical dislocation, and the brain was removed from the skull and the cerebral cortical tissue was removed from both hemispheres and rapidly frozen. Protein was extracted by homogenizing the samples in RIPA buffer with protease inhibitor (Pierce). The samples were left on ice for 30 min before centrifugation at 10,000 g at 4°C for a further 30 min. Supernatant w as removed and aliquoted before storage at −80°C. Protein concentration was determined using a bicinchoninic acid (BCA) assay using bovine serum albumin standards (Pierce). Proteins in 200 μg of total protein lysate were separated on a mini-protean®TGX™ gradient (4–15%) gel (Bio-Rad) at 100V for 120 min. Proteins in the gel were transferred electrophoretically to a Novex® PVDF 0.2 μm membrane (life science) at 4°C at 30V. Membranes were blocke d in 5% milk protein for 60 min at room temperature followed by overnight incubation with primary antibody (1:1000 dilutions) at 4°C. Primary antibodies used were: anti-Xrcc1 (Cell Signaling, Cat # 2735S); anti-NEIL1 (Santa Cruz, SC-134547); anti-DNA ligase III (BD Biosciences, Cat # 611876); anti-Caspase-3 (Cell Signaling, Cat #9662); and anti-β-actin (Santa Cruz, SC-1616). After washing the membrane, it was incubated in the presence of secondary (1:10000) for 120 min at room temperature. Secondary HRP conjugate was detected by chemiluminescence (Super Signal West Femto, Pierce) on a chemidoc imager XRS+™ (Bio-Rad). Images were analyzed and quantitated using ImageLab (V3.0) (Bio-Rad) with protein of interest signal normalized to -β-Actin signal.

2.6. TUNEL Staining, Microscopy, and Quantification

To evaluate apoptosis, TUNEL staining was performed on brain sections using a Deadend kit (Promega). Multiple sections from individual brain samples were layered on a glass slide

before the TUNEL assay; brain sections were fixed in 4% (vol/vol) paraformaldehyde and permeablized with 0.2% Triton X-100 and proteinase K as per manufacturer's instructions. After staining, the sections were mounted in hardset Vectashield medium containing DAPI. Additional staining was done with hematoxylin–eosin to locate the boundary of the ischemic penumbra (Borlongan, et al., 2000). The sections were photographed using a fluorescence microscope equipped with AxioVision software. Four wild type and four Xrcc1$^{+/-}$ brains were analyzed without knowledge of the genotype of the mice. A minimum of four microscopic fields within the ischemic penumbra of each section were photographed. TUNEL+ cells were counted in a double-blinded manner in each of these areas. An average of all of the TUNEL+ cells from these areas counted was taken from each brain section (Khan, et al., 2009). Data were analyzed by Student's two-tailed t-test.

2.7. Human brain samples and source

Human autopsy brain samples stored within 24 hours after death (n=18) were obtained from the Human Brain and Spinal Fluid Resource Center, VA West Los Angeles Healthcare Center, Los Angeles, CA 90073 which is sponsored by NINDS/NIMH, National Multiple Sclerosis Society, and Department of Veterans Affairs. All samples were taken from the parietal cortex region. Nine samples were from stroke victims and nine samples were from individuals whose death was attributed to non-neurological causes. Patient data are shown in Table 1.

2.8. Oligonucleotide substrates

All PAGE purified oligonucleotides were ordered from IDT (San Diego, CA). The oligonucleotide sequences and location of the specific lesions can be found in Table 2.

2.9. Preparation of brain tissue lysates

Human and mouse tissue lysates were prepared as described previously (Weissman, et al., 2007). Briefly, brain tissue lysates were prepared by homogenizing with a dounce homogenizer in buffer (20 mM Hepes, pH 7.5, 50 mM KCl, 2 mM EGTA and complete protease inhibitor (Roche). Lysates were centrifuged at 800 × g for 10 min to remove large cell debris. The resulting lysates were resuspended (2 mg/mL) in 20 mM Hepes (pH 7.0), 150 mM KCl, 2 mM EGTA, 1% (wt/vol) CHAPSO (Sigma-Aldrich), and protease inhibitor mixture and incubated at 4 °C for 1 h wit h end-over-end rotation. The lysates were centrifuged at 100,000 × g for 1 h, and the supernatants were collected. The samples were flash frozen in liquid nitrogen and stored at −80 °C unti l use. Protein concentration was determined using the BCA assay kit (Pierce).

2.10. Incision assays

Incision assays were performed as described previously (Weissman, et al., 2007). Briefly, incision reactions contained 100 fmol of ^{32}P-labeled duplex oligonucleotide with a specific modification. Samples were diluted in 10 mM HEPES–KOH (pH 7.4) containing 100 mM KCl. Reactions (10 μl) contained 25 mM HEPES–KOH (pH 7.4), 25 mM KCl, 0.1 mg/ml BSA, 5 mM $MgCl_2$, 10% glycerol, 0.05% Triton X-100 and different amount of protein. The reactions were incubated with whole tissue lysates at 32 °C. The incubation times and

amount of tissue lysate varied for each type of activity assay. While assaying for abasic site analog tetrahydrofuran cleavage, we incubated with 2 μg of whole tissue lysates for 5 minutes, whereas 60 μg of whole tissue lysates was incubated overnight when assaying for thymine glycol incision in the same lysates. The reactions were terminated by the addition of 5 mg/mL proteinase K and 10% SDS and incubated at 37 °C for 30 minutes follo wed by the addition of formamide-containing buffer and continued incubation at 95 °C for 5 minutes. These samples were resolved on a denaturing 15% polyacrylamide gel containing 7M urea then exposed to a phosphorimager screen. The gels were visualized by the Typhoon Phosphorimager (Molecular Dynamics, GE Healthcare, Ramsey, MN, USA). The images were analyzed using ImageQuant 5.2 software (GE Healthcare, Pittsburgh, PA, USA). The percent incision was calculated by dividing the product band intensity by the total intensity in the lane.

2.11. Incorporation assay

Single-nucleotide gap-filling reaction was performed as described previously (Canugovi, et al., 2014) using an unlabeled DNA oligo substrate with a single gap in the middle of the substrate (Table 2). Samples were diluted in 10 mM Tris-HCl (pH 7.4) containing 100 mM KCl to achieve similar protein concentrations in each of the independent samples. Reactions (10 μl) contained 50 mM Tris-HCl (pH 7.4), 50 mM KCl, 1 mM dithiothreitol (DTT), 5 mM $MgCl_2$, 5% glycerol, 5 mM deoxycytidinetriphosphate (dCTP) (Roche Applied Sciences, Indianapolis, IN, USA), 1 pmol of duplex gap oligonucleotide, 4 μCi of ^{32}P-dCTP (GE Healthcare, Pittsburgh, PA, USA), and 40 μg protein. Reactions were incubated at 37 °C for 3 hours and terminated by the addition of 1 μL of 0.5M ethylenediaminetetraacetic acid (EDTA) and formamide dye followed by the heating at 95 °C for 5 minutes. Samples were resolved on a polyacrylamide gel as described above.

2.12. Immunodetection of XRCC1 and NEIL1 in postmortem human brain tissue

Multiple sections from a single brain were layered on a glass slide, fixed in 4% (vol/vol) formaldehyde for 20 min, and air dried overnight at 4 °C. Slides wer e rehydrated, microwaved in 0.1 M citrate buffer (pH 6) for 10 min, and gradually allowed to cool to room temperature. Slides were washed twice in PBS and blocked for 1 h with 5% goat serum in PBS. Antibodies were diluted (1:200) in 5% goat serum in PBS. Tissue sections were incubated with primary antibodies for overnight at 4 °C, washed three times with PBS and incubated with diluted secondary antibody for 90 min at room temperature. Samples were rinsed and mounted in Vector shield hard set with DAPI. Sections were photographed using a fluorescence microscope equipped with AxioVision software. The primary antibodies used were rabbit Anti-*Xrcc1* (Cell Signaling, Cat # 2735S) and rabbit Anti-Neil1 (Santa Cruz, SC-134547). Alexa Fluor 488 goat anti-rabbit IgG was used as the secondary antibody (Molecular Probe, USA).

2.13. Hexokinase Assay

Human brain tissue lysates were prepared and hexokinase activities in the brain tissue were determined as per manufacturer instruction (Hexokinase Colorimetric Assay Kit, Sigma Cat # MAK091).

2.14. Statistics

When comparing the means (or medians) of two independent samples, a two-sample Student's *t*-test was used (or the nonparametric Mann–Whitney test). When comparing the means (or medians) among a number of independent samples, a one-way analysis of variance (ANOVA) was used (or the nonparametric Kruskal–Wallis test). In the experiments where each animal was measured on three occasions (pre-stroke and at 24 and 48 h after stroke), a randomized complete block design was applied to account for the repeated measures on the animals (this is equivalent to a two-sample ANOVA with no interaction term). Appropriate post hoc approaches, as mentioned in the results section were conducted to control the false positive error rate. A 5% significance level is used throughout. Graphpad Prism version 5 and Statistical Aanalysis System (SAS) programming were used to calculate statistics in various experiments.

For analyzing human data, the results are reported as mean ± standard error. Each assay was performed at least twice (on 9 independent biological samples per set). The differences among human control and stroke samples were analyzed by the Student's *t*-test, and a $p < 0.05$ was considered statistically significant.

3. Results

3.1. *Xrcc1* $^{+/-}$ mice exhibit greater brain damage, increased mortality, and poorer functional recovery after ischemic stroke

To study the role of Xrcc1 and BER in brain cells subjected to severe stress, we performed middle cerebral artery occlusion/reperfusion (MCAO/R) on 12 wild type (WT) and 14 *Xrcc1* $^{+/-}$ mice at 12 months of age. Post-stroke mortality rate, infarct volume, and neurological deficits were measured in each case. The infarct volume was measured in brains of mice that were alive at 48 h after stroke by TTC staining, and neurological deficits were assessed for these mice as described in the materials and methods section (n = 6 each). The infarct volume was significantly higher in *Xrcc1* $^{+/-}$ mice compared with WT mice (37.2 ± 2.7% for WT and 50.9 ± 3.1% for Xrcc1 $^{+/-}$, $p<0.01$) as determined by the Mann–Whitney test (Fig. 1A and B). The observed mortality rate was about 2.2-fold higher in *Xrcc1* $^{+/-}$ mice (35.7%) compared to WT mice (16.6%) after ischemic stroke, although it did not reach statistical significance (Fig. 1C). Furthermore, the neurological deficit score was increased significantly in *Xrcc1* $^{+/-}$ mice relative to WT mice ($p<0.05$) at both 24 and 48 h post-stroke (Fig. 1D).

3.2. Impaired motor function in *Xrcc1*$^{+/-}$ mice after ischemic stroke

Stroke patients are prone to partial or complete loss of motor function, clinically known as paralysis. This is mainly attributed to the degeneration of cortical motor neurons (and/or their axons in their subcortical course) caused by mechanisms involving excess oxidative stress, DNA damage, and apoptosis (Broughton, et al., 2009,Niizuma, et al., 2009). To study the effect of partial loss of Xrcc1 on motor function after ischemic stroke, rotarod tests were performed at 24 and 48 h after stroke in WT (n = 4) and *Xrcc1* $^{+/-}$ (n = 4, age =5–6 months) mice. Prior to stroke, *Xrcc1*$^{+/-}$ mice did not show any difference on the rotarod test relative to WT mice (Fig. 2), consistent with the previous findings (McNeill, et al., 2011). However,

at both the 24 and 48 h time points after stroke, the measured number of falls during the rotarod tests was significantly higher in *Xrcc1* $^{+/-}$ mice compared to WT mice (Fig. 2A). Indeed, our studies indicate that WT mice appear to recover completely as assessed by number of falls post-stroke by 48 h, whereas *Xrcc1* $^{+/-}$ mice still exhibit profound deficits at that time point. A second parameter, latency to the first fall, which measures motor coordination and grip strength, was also significantly reduced and showed an impaired rate of recovery in *Xrcc1* $^{+/-}$ mice after MCAO/R (Fig. 2B). These data suggest that the partial loss of Xrcc1 in mice exacerbates stroke-induced motor dysfunction.

3.3. Partial loss of Xrcc1 results in enhanced apoptosis in brain cells of mice subjected to stroke

Previous data show that Xrcc1 haploinsufficiency does not cause adverse phenotypic changes under normal conditions, in terms of life expectancy, weight, body fat composition, organ function, motor coordination, brain integrity or memory, bone marrow cellularity, blood cell composition or morphology, and chromosome status (McNeill, et al., 2011). However, these mice were sensitive to the exogenous genotoxin azoxymethane, an alkylating agent that causes DNA damage (McNeill, et al., 2011). Here, we used stroke to induce oxidative stress, which could in turn generate increased levels of DNA lesions that trigger apoptosis in cells. We determined the impact of the reduced DNA repair capacity in *Xrcc1* $^{+/-}$ mice on the vulnerability of neurons in the ischemic penumbra to apoptosis. A terminal deoxynucleotidyl transferase (TdT) dUTP nick end-labeling (TUNEL) assay was performed on brain sections from *Xrcc1* $^{+/-}$ and WT mice (n=4) at 48 h after focal ischemia/reperfusion. Data were analyzed by a two-tailed Student's *t*-test, and revealed that there were significantly more TUNEL+ cells in the ischemic penumbra of *Xrcc1* $^{+/-}$ mice compared with WT mice (Fig. 3A and B). Consistently, protein markers of apoptosis including cleaved caspase-3 (sum of p17 and p19 fragments) were increased and full length caspase 3 was decreased in the brain lysates of *Xrcc1* $^{+/-}$ mice compared with WT mice (Fig. 3C), indicating that partial loss of Xrcc1 renders brain cells vulnerable to apoptosis following a stroke. There was no observable increase in TUNEL+ cells in the brain tissue from the nonischemic (contralateral) cerebral hemispheres of *Xrcc1* $^{+/-}$ mice in comparison to WT mice, as there were no TUNEL+ cells in either sample (Fig. S1A).Moreover, there was no difference in the level of cleaved caspase 3 in the brain tissue from the nonischemic (contralateral) cerebral hemispheres of WT and *Xrcc1* $^{+/-}$ mice (data not shown).

3.4. Post stroke brain samples from *Xrcc1* $^{+/-}$ mice show loss of DNA ligase III expression and reduced DNA repair capacity

To further characterize the above observation, whole cell lysates were prepared from ipsilateral (ischemic) and contralateral (non-ischemic) cerebral cortex of WT and *Xrcc1* $^{+/-}$ mice 48 h after MCAO/R, and the lysates were subsequently analyzed for the expression of Xrcc1 and DNA Lig3 by immunoblotting. In addition, BER synthesis and ligation was measured in prepared lysates using a 91-mer double-strand substrate containing a single nucleotide gap and radiolabeled dCTP nucleotides. For the contralateral side, immunoblotting revealed half the signal for Xrcc1, whereas there was no change in Lig3 levels in brain tissue from the non-ischemic cerebral hemispheres of *Xrcc1* $^{+/-}$ mice (Fig. 4A). Furthermore, levels of BER activity were similar in tissue from the contralateral

cerebral hemispheres of WT and *Xrcc1* $^{+/-}$ mice (Fig. 4B and Fig. S1B). On the ipsilateral side, Xrcc1 and Lig3 levels were lower in *Xrcc1* $^{+/-}$ mice relative to WT mice (Fig. 4C). Moreover, BER activity in whole cell lysates of cerebral cortex tissue in the ischemic penumbra of *Xrcc1* $^{+/-}$ mice was significantly reduced compared to WT mice (58% lower in *Xrcc1* $^{+/-}$ mice than WT mice, Fig. 4D and Fig. S1B).

Together, these results suggest that the slightly reduced protein level of Xrcc1 has no effect on overall Lig3 levels or BER activity in the nonischemic brain region (contralateral part). Conversely, the overall protein level of Xrcc1 appears to be more important in the induction/stability of Lig3 and BER capacity in the brain cells (ipsilateral part) that are challenged with acute ischemic stroke.

3.5. Impaired BER activities in postmortem human brain tissue samples from individuals who died of stroke

The data presented so far indicate the importance of BER capacity in recovering from focal ischemic stroke in mice. We wondered if altered BER activities might be seen in human stroke patients. Although population studies predicted that loss or modifications of BER players such as OGG1 or XRCC1 might enhance vulnerability to stroke (Dutra, et al., 2006,Mahabir, et al., 2007,Shyu, et al., 2012), detailed biochemical analysis has not been reported. Hence, we determined the capacity of specific BER steps in extracts prepared from human post-mortem cerebral cortical tissue samples from individuals who had died from stroke as well as individuals who had died of non-neurological causes (Table 1). DNA glycosylase activity was assayed by the incision of a radiolabeled DNA oligonucleotide substrate containing a single lesion, thymine glycol, and an oligonucleotide containing the abasic site analog THF was used to measure AP site incision activity. Incision activity was calculated as the amount of radioactivity in the band corresponding to the damage-specific cleavage product over the total radioactivity in the lane. Interestingly, lysates from the stroke affected brain regions showed significantly reduced thymine glycol incision (42.76 ± 11.01 % vs 52.97 ± 6.67 %, p-value 0.031) and AP endonuclease activity (34.51 ± 11.14 % versus 48.31 ± 10.24 %, p-value 0.037) (Fig. 5A and 5B). We have also checked the excision of 5-hydroxy uracil (5-OHU), the preferred substrate for NEIL1 but the activity was found too low for quantitative analysis (data not shown). We then assayed for whole BER activity, as described above. Whole BER activity was 27% lower in stroke samples than in control samples ($P = 0.027$) (Fig. 5C).

The postmortem intervals (PMIs) of the samples used in this study averaged 14.9 hours in stroke patients and 12.7 hours in control brains. To eliminate the possibility of loss of activity due to stroke itself or storage conditions we performed enzymatic assays on one of the constitutively expressed enzymes in brain, hexokinase. We found no significant differences in the protein's activity in the sample groups (Fig. S2). Moreover, we plotted the PMI against each of the assays for all samples to determine if there was any correlation in activity to the length of PMI. No correlation was found between length of PMI and repair activities (Fig. S3). These results are consistent with our prior study where a similar analysis had been done (Canugovi, et al., 2014).

3.6. Reduced expression of XRCC1, NEIL1 and DNA LIG3 proteins in human brain samples derived from individuals who died of stroke

We wondered whether the loss of the BER activities described above related to a loss of protein expression. Since NEIL1 plays an important role and serves as back-up glycosylase (Hazra, et al., 2002,Katafuchi, et al., 2004,Takao, et al., 2002) in the initial steps of BER. DNA LIG3 and XRCC1 plays a crucial role in later steps of BER, it was of interest to study the expression of these three proteins in stroke affected human brains compared to controls. To examine this, we utilized immunoblotting and immunofluorescence methods. In both cases, we found significantly lower XRCC1 expression (51% lower, P = 0.020) in the human stoke brain samples compared to control brain samples (Fig. 6A and B) and lower expression of DNA LIG3 in the human stroke patient brain samples compared to control brain samples (Fig. S4). Similarly, we also found a significant loss of NEIL1, a major DNA glycosylase that removes oxidative damage from DNA (54% lower, P=0.004, Fig. 7A and B). Together, these data suggest that there may be significantly less BER activity in stroke postmortem brain samples.

4. Discussion

In this study, we provide evidence that effective and efficient BER is essential for speedy recovery from stroke. Specifically, we found that heterozygous *Xrcc1* mice recover poorly from stroke as compared to wild type littermates. Importantly, reduced DNA repair capacity in heterozygous *Xrcc1* mice was sufficient to trigger higher cellular death in the ischemic penumbra. These observations underscore the importance of robust BER for recovery of mice from stroke. To extend our analysis to human subjects, we investigated BER capacity in stroke-affected human post-mortem brain samples and compared them with human brain autopsy samples from individuals who had died of non-neurological causes. The results indicate that stroke is associated with a significant impairment of general BER function and reduced expression of XRCC1 and NEIL1. These findings suggest that effective BER is likely important for recovery from stroke.

XRCC1 is a non-enzymatic scaffold protein that plays critical roles in BER and SSBR. In mouse models, loss or dysfunction of both alleles of *Xrcc1* causes death at embryonic stages E6.5–7.5, due to abnormal development of the embryonic endoderm (Tebbs, et al., 1999). In addition, published data links functional defects in XRCC1 with neurodegenerative diseases and cancer (Caldecott, 2008,Ladiges, 2006,Wilson, et al., 2011). Therefore, heterozygous and other hypomorphic *Xrcc1* mouse strains are a useful system for investigating the in vivo biological role(s) of XRCC1.

Initial characterization of $Xrcc1^{+/-}$ heterozygous mice demonstrated that the phenotypic consequences of copy number reduction of *Xrcc1* are relatively minor in the absence of exogenous stressors (McNeill, et al., 2011). Mice with one functional allele of *Xrcc1* have no prominent neurological defects during development and display normal cognitive ability as adult mice. Minor neurological defects have been noted in some adult $Xrcc1^{+/-}$ animals and a few a animals exhibited behavioral features commonly associated with stroke (McNeill, et al., 2011). Furthermore, specific inactivation of both alleles of *Xrcc1* in the nervous system of adult mice contributes to neuropathology including loss of cerebellar

interneurons, abnormal hippocampal neurons, progressive mild ataxia and episodic spasms (Lee, et al., 2009). These data support the idea that Xrcc1 plays an important role in neurons in immature and mature mice. However, ectopic expression of a small amount (<10% the normal level) of wild type *Xrcc1* fully complements the developmental defect in *Xrcc1* null embryos and reverses sensitivity to DNA damaging agents in *Xrcc1* null fibroblasts (Tebbs, et al., 1999). Therefore, it is reasonable to propose that under some conditions, one functional allele of *Xrcc1* is adequate for normal functions of the cell, while under other conditions, likely involving stress, higher levels of *Xrcc1* expression may be required to prevent such damage. The data presented in this paper are fully consistent with this hypothesis.

Two human population studies revealed that polymorphisms in BER genes APE1 and XRCC1 had no association with large artery atherosclerotic (LAA) stroke (Dutra, et al., 2006,Mahabir, et al., 2007). A second population study involving cigarette smoking and non-smoking groups showed that polymorphisms of ERCC2 and XPD were associated with LAA stroke risk, and expression of both OGG1 and ERCC2 polymorphisms concurrently elevated the risk of LAA stroke; additionally, this risk was elevated with cigarette smoking in all groups (Shyu, et al., 2012). Although there is no association of APE/ref-1, XRCC1, OGG1 gene polymorphisms with stroke by themselves, combinations of these three polymorphisms increased the risk for LAA stroke in smokers, indicating the importance of efficient BER in an increased oxidative stress environment (Canugovi, et al., 2013).

It has been shown that Xrcc1 is one of the BER proteins that is upregulated with transient ischemia as part of cellular stress resistance mechanisms (Li, et al., 2007). However, we did not observe this as seen in western blots in Fig. 4, compare WT ipsilateral to contralateral. Additionally, we found that at 24 and 48 h after the stroke, mice having a single *Xrcc1* gene copy exhibited significantly poorer performance in the rotarod test assessing motor function than to wild type mice. This indicates that higher levels of Xrcc1 are essential for resistance to adverse effects caused by ischemic stroke and for a recovery after stroke.

The interpretation of above results is complicated by the fact that XRCC1 is required for the stability of Lig3, a DNA repair protein expressed in both mitochondrial and nuclear compartments whose function overlaps with, but is not redundant to, that of DNA ligases I and IV. Although XRCC1 and Lig3 play apparently independent roles in response to DNA damage in the nuclear and mitochondrial compartments, respectively (Lakshmipathy and Campbell, 2000), on the biochemical level, XRCC1 is required to stabilize and ensure the enzymatic competence of DNA Lig3 (Simsek, et al., 2011a,Simsek, et al., 2011b). In addition, XRCC1 interacts with and stimulates the function of other DNA repair proteins and pathways, supporting the hypothesis that XRCC1 increases the efficiency of the BER process, possibly more so when cells are challenged with oxidative stress.

Our data suggest that the partial loss of the important DNA repair protein, Xrcc1 renders brain cells susceptible to ischemic stroke and its robust action is critical in the survival of cells under conditions of severe oxidative stress. However, other factors in operation in stroke apart from oxidative stress may also contribute to the overall response. This is in agreement with previous studies showing that BER is a major pathway for the repair of

oxidatively modified DNA bases in neurons (Harrison, et al., 2005,Karahalil, et al., 2002). With regards to brain damage from stroke, our findings suggest that neurons that are better able to repair oxidative DNA lesions have an increased chance of survival, consistent with the previous studies of BER activity in mouse models of ischemic stroke (Canugovi, et al., 2012,Liu, et al., 2011). In a recent human study, it has been shown that there is little plasticity both in terms of neurogenesis or genomic rearrangements in human cortical neurons and the neurons having effective DNA repair system survived long-term after stroke (Huttner, et al., 2014). Since BER is important for mice to recover from focal ischemic stroke, we measured BER activities in brain specimens from patients that died of stroke or normal controls who died from non-neurological causes. . Our findings show that XRCC1 and NEIL1 protein levels were significantly lower in brains of stroke patients than in controls. Our findings are consistent with earlier studies where we have shown that a lower level of BER protein is associated with neurological diseases (Canugovi, et al., 2014,Weissman, et al., 2007). These findings, along with our prior publications (Canugovi, et al., 2012,Liu, et al., 2011) provide compelling evidence that BER capacity matters with respect to one's ability to recover from an acute ischemic event. Furthermore, as we enter the era of personalize medicine an individual's collective BER genotype may be useful to identify individuals as risk of poor recover from ischemic events.

Collectively, these results show that even a haploinsufficiency, and not a complete knockout, of a DNA repair gene is detrimental to brain cell survival after stroke. Together our data suggest that effective and efficient BER plays significant role in protecting cells from stroke-induced adverse effects.

Supplementary Material

Refer to Web version on PubMed Central for supplementary material.

Acknowledgments

This research was supported entirely by the Intramural Research Program of the National Institutes of Health and National Institute on Aging (AG 000723-07). We would like to thank Human Brain and Spinal Fluid Resource Center, VA West Los Angeles Healthcare Center, Los Angeles, CA 90073 which is sponsored by NINDS/NIMH, National Multiple Sclerosis Society, and Department of Veterans Affairs for the human postmortem brain samples used in this study. Additionally, we would like to thank Drs. Beverly A. Baptiste and Raghavendra A. Shamanna for critically reading the manuscript.

References

Arumugam TV, Phillips TM, Cheng A, Morrell CH, Mattson MP, Wan R. Age and energy intake interact to modify cell stress pathways and stroke outcome. Annals of neurology. 2010; 67(1):41–52. DOI: 10.1002/ana.21798 [PubMed: 20186857]

Bederson JB, Pitts LH, Tsuji M, Nishimura MC, Davis RL, Bartkowski H. Rat middle cerebral artery occlusion: evaluation of the model and development of a neurologic examination. Stroke; a journal of cerebral circulation. 1986; 17(3):472–6.

Borlongan CV, Yamamoto M, Takei N, Kumazaki M, Ungsuparkorn C, Hida H, Sanberg PR, Nishino H. Glial cell survival is enhanced during melatonin-induced neuroprotection against cerebral ischemia. FASEB journal : official publication of the Federation of American Societies for Experimental Biology. 2000; 14(10):1307–17. [PubMed: 10877823]

Broughton BR, Reutens DC, Sobey CG. Apoptotic mechanisms after cerebral ischemia. Stroke; a journal of cerebral circulation. 2009; 40(5):e331–9. DOI: 10.1161/STROKEAHA.108.531632

Caldecott KW. Single-strand break repair and genetic disease. Nature reviews Genetics. 2008; 9(8): 619–31. DOI: 10.1038/nrg2380

Caldecott KW, Aoufouchi S, Johnson P, Shall S. XRCC1 polypeptide interacts with DNA polymerase beta and possibly poly (ADP-ribose) polymerase, and DNA ligase III is a novel molecular 'nick-sensor' in vitro. Nucleic acids research. 1996; 24(22):4387–94. [PubMed: 8948628]

Campalans A, Marsin S, Nakabeppu Y, O'Connor TR, Boiteux S, Radicella JP. XRCC1 interactions with multiple DNA glycosylases: a model for its recruitment to base excision repair. DNA repair. 2005; 4(7):826–35. DOI: 10.1016/j.dnarep.2005.04.014 [PubMed: 15927541]

Canugovi C, Misiak M, Ferrarelli LK, Croteau DL, Bohr VA. The role of DNA repair in brain related disease pathology. DNA repair. 2013; 12(8):578–87. DOI: 10.1016/j.dnarep.2013.04.010 [PubMed: 23721970]

Canugovi C, Shamanna RA, Croteau DL, Bohr VA. Base excision DNA repair levels in mitochondrial lysates of Alzheimer's disease. Neurobiology of aging. 2014; 35(6):1293–300. DOI: 10.1016/j.neurobiolaging.2014.01.004 [PubMed: 24485507]

Canugovi C, Yoon JS, Feldman NH, Croteau DL, Mattson MP, Bohr VA. Endonuclease VIII-like 1 (NEIL1) promotes short-term spatial memory retention and protects from ischemic stroke-induced brain dysfunction and death in mice. Proceedings of the National Academy of Sciences of the United States of America. 2012; 109(37):14948–53. DOI: 10.1073/pnas.1204156109 [PubMed: 22927410]

Date H, Onodera O, Tanaka H, Iwabuchi K, Uekawa K, Igarashi S, Koike R, Hiroi T, Yuasa T, Awaya Y, Sakai T, Takahashi T, Nagatomo H, Sekijima Y, Kawachi I, Takiyama Y, Nishizawa M, Fukuhara N, Saito K, Sugano S, Tsuji S. Early-onset ataxia with ocular motor apraxia and hypoalbuminemia is caused by mutations in a new HIT superfamily gene. Nature genetics. 2001; 29(2):184–8. DOI: 10.1038/ng1001-184 [PubMed: 11586299]

Dutra AV, Lin HF, Juo SH, Mohrenweiser H, Sen S, Grewal RP. Analysis of the XRCC1 gene as a modifier of the cerebral response in ischemic stroke. BMC medical genetics. 2006; 7:78.doi: 10.1186/1471-2350-7-78 [PubMed: 17087834]

Harrison JF, Hollensworth SB, Spitz DR, Copeland WC, Wilson GL, LeDoux SP. Oxidative stress-induced apoptosis in neurons correlates with mitochondrial DNA base excision repair pathway imbalance. Nucleic acids research. 2005; 33(14):4660–71. DOI: 10.1093/nar/gki759 [PubMed: 16107556]

Hazra TK, Izumi T, Boldogh I, Imhoff B, Kow YW, Jaruga P, Dizdaroglu M, Mitra S. Identification and characterization of a human DNA glycosylase for repair of modified bases in oxidatively damaged DNA. Proceedings of the National Academy of Sciences of the United States of America. 2002; 99(6):3523–8. DOI: 10.1073/pnas.062053799 [PubMed: 11904416]

Huttner HB, Bergmann O, Salehpour M, Racz A, Tatarishvili J, Lindgren E, Csonka T, Csiba L, Hortobagyi T, Mehes G, Englund E, Solnestam BW, Zdunek S, Scharenberg C, Strom L, Stahl P, Sigurgeirsson B, Dahl A, Schwab S, Possnert G, Bernard S, Kokaia Z, Lindvall O, Lundeberg J, Frisen J. The age and genomic integrity of neurons after cortical stroke in humans. Nature neuroscience. 2014; 17(6):801–3. DOI: 10.1038/nn.3706 [PubMed: 24747576]

Karahalil B, Hogue BA, de Souza-Pinto NC, Bohr VA. Base excision repair capacity in mitochondria and nuclei: tissue-specific variations. FASEB journal : official publication of the Federation of American Societies for Experimental Biology. 2002; 16(14):1895–902. DOI: 10.1096/fj.02-0463com [PubMed: 12468454]

Katafuchi A, Nakano T, Masaoka A, Terato H, Iwai S, Hanaoka F, Ide H. Differential specificity of human and Escherichia coli endonuclease III and VIII homologues for oxidative base lesions. The Journal of biological chemistry. 2004; 279(14):14464–71. DOI: 10.1074/jbc.M400393200 [PubMed: 14734554]

Khan M, Im YB, Shunmugavel A, Gilg AG, Dhindsa RK, Singh AK, Singh I. Administration of S-nitrosoglutathione after traumatic brain injury protects the neurovascular unit and reduces secondary injury in a rat model of controlled cortical impact. Journal of neuroinflammation. 2009; 6:32.doi: 10.1186/1742-2094-6-32 [PubMed: 19889224]

Kulkarni A, McNeill DR, Gleichmann M, Mattson MP, Wilson DM 3rd. XRCC1 protects against the lethality of induced oxidative DNA damage in nondividing neural cells. Nucleic acids research. 2008; 36(15):5111–21. DOI: 10.1093/nar/gkn480 [PubMed: 18682529]

Ladiges WC. Mouse models of XRCC1 DNA repair polymorphisms and cancer. Oncogene. 2006; 25(11):1612–9. DOI: 10.1038/sj.onc.1209370 [PubMed: 16550161]

Lakshmipathy U, Campbell C. Mitochondrial DNA ligase III function is independent of Xrcc1. Nucleic acids research. 2000; 28(20):3880–6. [PubMed: 11024166]

Lee Y, Katyal S, Li Y, El-Khamisy SF, Russell HR, Caldecott KW, McKinnon PJ. The genesis of cerebellar interneurons and the prevention of neural DNA damage require XRCC1. Nature neuroscience. 2009; 12(8):973–80. DOI: 10.1038/nn.2375 [PubMed: 19633665]

Li N, Wu H, Yang S, Chen D. Ischemic preconditioning induces XRCC1, DNA polymerase-beta, and DNA ligase III and correlates with enhanced base excision repair. DNA repair. 2007; 6(9):1297–306. DOI: 10.1016/j.dnarep.2007.02.027 [PubMed: 17412650]

Liu D, Croteau DL, Souza-Pinto N, Pitta M, Tian J, Wu C, Jiang H, Mustafa K, Keijzers G, Bohr VA, Mattson MP. Evidence that OGG1 glycosylase protects neurons against oxidative DNA damage and cell death under ischemic conditions. Journal of cerebral blood flow and metabolism : official journal of the International Society of Cerebral Blood Flow and Metabolism. 2011; 31(2):680–92. DOI: 10.1038/jcbfm.2010.147

Mahabir S, Abnet CC, Qiao YL, Ratnasinghe LD, Dawsey SM, Dong ZW, Taylor PR, Mark SD. A prospective study of polymorphisms of DNA repair genes XRCC1, XPD23 and APE/ref-1 and risk of stroke in Linxian, China. Journal of epidemiology and community health. 2007; 61(8):737–41. DOI: 10.1136/jech.2006.048934 [PubMed: 17630376]

Mani RS, Fanta M, Karimi-Busheri F, Silver E, Virgen CA, Caldecott KW, Cass CE, Weinfeld M. XRCC1 stimulates polynucleotide kinase by enhancing its damage discrimination and displacement from DNA repair intermediates. The Journal of biological chemistry. 2007; 282(38): 28004–13. DOI: 10.1074/jbc.M704867200 [PubMed: 17650498]

Marintchev A, Robertson A, Dimitriadis EK, Prasad R, Wilson SH, Mullen GP. Domain specific interaction in the XRCC1-DNA polymerase beta complex. Nucleic acids research. 2000; 28(10): 2049–59. [PubMed: 10773072]

Marsin S, Vidal AE, Sossou M, Menissier-de Murcia J, Le Page F, Boiteux S, de Murcia G, Radicella JP. Role of XRCC1 in the coordination and stimulation of oxidative DNA damage repair initiated by the DNA glycosylase hOGG1. The Journal of biological chemistry. 2003; 278(45):44068–74. DOI: 10.1074/jbc.M306160200 [PubMed: 12933815]

McNeill DR, Lin PC, Miller MG, Pistell PJ, de Souza-Pinto NC, Fishbein KW, Spencer RG, Liu Y, Pettan-Brewer C, Ladiges WC, Wilson DM 3rd. XRCC1 haploinsufficiency in mice has little effect on aging, but adversely modifies exposure-dependent susceptibility. Nucleic acids research. 2011; 39(18):7992–8004. DOI: 10.1093/nar/gkr280 [PubMed: 21737425]

Moreira MC, Barbot C, Tachi N, Kozuka N, Uchida E, Gibson T, Mendonca P, Costa M, Barros J, Yanagisawa T, Watanabe M, Ikeda Y, Aoki M, Nagata T, Coutinho P, Sequeiros J, Koenig M. The gene mutated in ataxia-ocular apraxia 1 encodes the new HIT/Zn-finger protein aprataxin. Nature genetics. 2001; 29(2):189–93. DOI: 10.1038/ng1001-189 [PubMed: 11586300]

Mortusewicz O, Leonhardt H. XRCC1 and PCNA are loading platforms with distinct kinetic properties and different capacities to respond to multiple DNA lesions. BMC molecular biology. 2007; 8:81.doi: 10.1186/1471-2199-8-81 [PubMed: 17880707]

Niizuma K, Endo H, Chan PH. Oxidative stress and mitochondrial dysfunction as determinants of ischemic neuronal death and survival. Journal of neurochemistry. 2009; 109(Suppl 1):133–8. DOI: 10.1111/j.1471-4159.2009.05897.x [PubMed: 19393019]

Shyu HY, Shieh JC, Ji-Ho L, Wang HW, Cheng CW. Polymorphisms of DNA repair pathway genes and cigarette smoking in relation to susceptibility to large artery atherosclerotic stroke among ethnic Chinese in Taiwan. Journal of atherosclerosis and thrombosis. 2012; 19(4):316–25. [PubMed: 22277767]

Simsek D, Brunet E, Wong SY, Katyal S, Gao Y, McKinnon PJ, Lou J, Zhang L, Li J, Rebar EJ, Gregory PD, Holmes MC, Jasin M. DNA ligase III promotes alternative nonhomologous end-joining during chromosomal translocation formation. PLoS genetics. 2011a; 7(6):e1002080.doi: 10.1371/journal.pgen.1002080 [PubMed: 21655080]

Simsek D, Furda A, Gao Y, Artus J, Brunet E, Hadjantonakis AK, Van Houten B, Shuman S, McKinnon PJ, Jasin M. Crucial role for DNA ligase III in mitochondria but not in Xrcc1-dependent repair. Nature. 2011b; 471(7337):245–8. DOI: 10.1038/nature09794 [PubMed: 21390132]

Swanson RA, Sharp FR. Infarct measurement methodology. Journal of cerebral blood flow and metabolism : official journal of the International Society of Cerebral Blood Flow and Metabolism. 1994; 14(4):697–8. DOI: 10.1038/jcbfm.1994.88

Takao M, Kanno S, Kobayashi K, Zhang QM, Yonei S, van der Horst GT, Yasui A. A back-up glycosylase in Nth1 knock-out mice is a functional Nei (endonuclease VIII) homologue. The Journal of biological chemistry. 2002; 277(44):42205–13. DOI: 10.1074/jbc.M206884200 [PubMed: 12200441]

Takashima H, Boerkoel CF, John J, Saifi GM, Salih MA, Armstrong D, Mao Y, Quiocho FA, Roa BB, Nakagawa M, Stockton DW, Lupski JR. Mutation of TDP1, encoding a topoisomerase I-dependent DNA damage repair enzyme, in spinocerebellar ataxia with axonal neuropathy. Nature genetics. 2002; 32(2):267–72. DOI: 10.1038/ng987 [PubMed: 12244316]

Taylor RM, Wickstead B, Cronin S, Caldecott KW. Role of a BRCT domain in the interaction of DNA ligase III-alpha with the DNA repair protein XRCC1. Current biology : CB. 1998; 8(15):877–80. [PubMed: 9705932]

Tebbs RS, Flannery ML, Meneses JJ, Hartmann A, Tucker JD, Thompson LH, Cleaver JE, Pedersen RA. Requirement for the Xrcc1 DNA base excision repair gene during early mouse development. Developmental biology. 1999; 208(2):513–29. DOI: 10.1006/dbio.1999.9232 [PubMed: 10191063]

Tomkinson AE, Vijayakumar S, Pascal JM, Ellenberger T. DNA ligases: structure, reaction mechanism, and function. Chemical reviews. 2006; 106(2):687–99. DOI: 10.1021/cr040498d [PubMed: 16464020]

Vidal AE, Boiteux S, Hickson ID, Radicella JP. XRCC1 coordinates the initial and late stages of DNA abasic site repair through protein-protein interactions. The EMBO journal. 2001; 20(22):6530–9. DOI: 10.1093/emboj/20.22.6530 [PubMed: 11707423]

Weissman L, Jo DG, Sorensen MM, de Souza-Pinto NC, Markesbery WR, Mattson MP, Bohr VA. Defective DNA base excision repair in brain from individuals with Alzheimer's disease and amnestic mild cognitive impairment. Nucleic acids research. 2007; 35(16):5545–55. DOI: 10.1093/nar/gkm605 [PubMed: 17704129]

Whitehouse CJ, Taylor RM, Thistlethwaite A, Zhang H, Karimi-Busheri F, Lasko DD, Weinfeld M, Caldecott KW. XRCC1 stimulates human polynucleotide kinase activity at damaged DNA termini and accelerates DNA single-strand break repair. Cell. 2001; 104(1):107–17. [PubMed: 11163244]

Wilson DM 3rd, Kim D, Berquist BR, Sigurdson AJ. Variation in base excision repair capacity. Mutation research. 2011; 711(1–2):100–12. DOI: 10.1016/j.mrfmmm.2010.12.004 [PubMed: 21167187]

Wilson DM 3rd, Mattson MP. Neurodegeneration: nicked to death. Current biology : CB. 2007; 17(2):R55–8. DOI: 10.1016/j.cub.2006.12.012 [PubMed: 17240329]

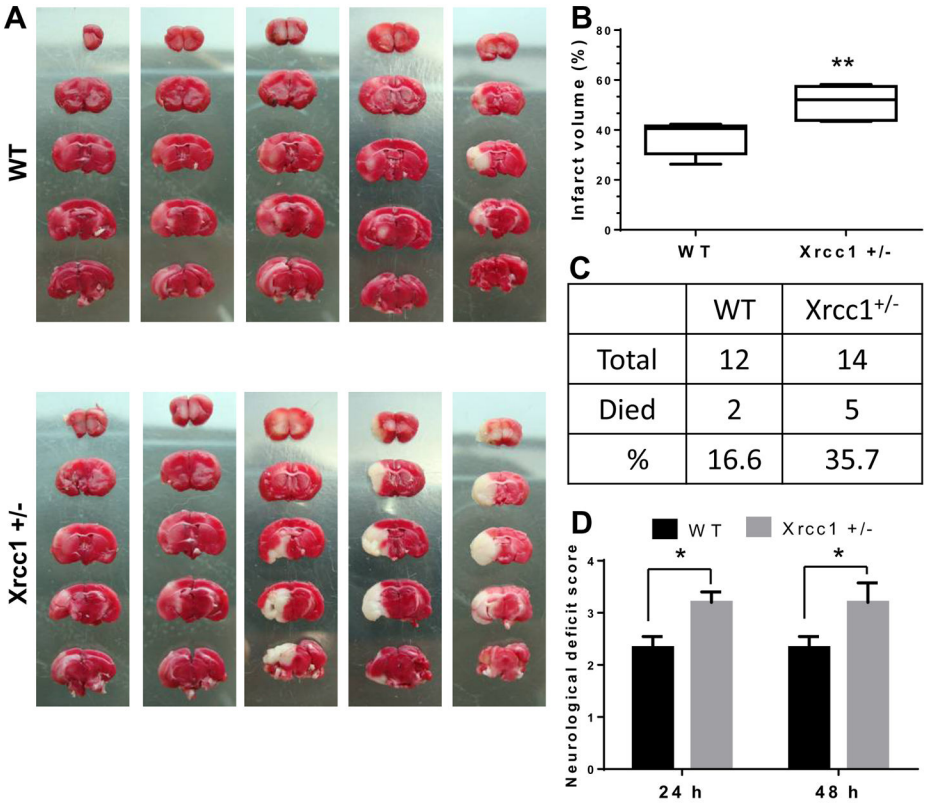

	WT	Xrcc1$^{+/-}$
Total	12	14
Died	2	5
%	16.6	35.7

Figure 1.

Infarct volume, mortality rate, and neurological deficit after middle cerebral artery occlusion/ reperfusion (MCAO/R) in WT and *Xrcc1* $^{+/-}$ mice. (A) Mouse brain sections stained with 2,3,5-triphenyltetrazolium chloride (TTC) after 48 h of MCAO/R. (B) Quantification of the infarct volume shown in A. The data are presented as a box plot diagram, which represents the minimum to maximum distribution of the average percentage of infarct volume ± SEM. (C) Percentage of death in mice within 48 h of the MCAO/R procedure. (D) Graphic of the assigned neurological deficit score at 24 and 48 h after the MCAO/R procedure. Data are presented as means ± SEM. Statistical analysis was performed by one-way ANOVA followed by Bonferroni's post-hoc test for pairwise comparisons, *p<0.05, **p<0.01.

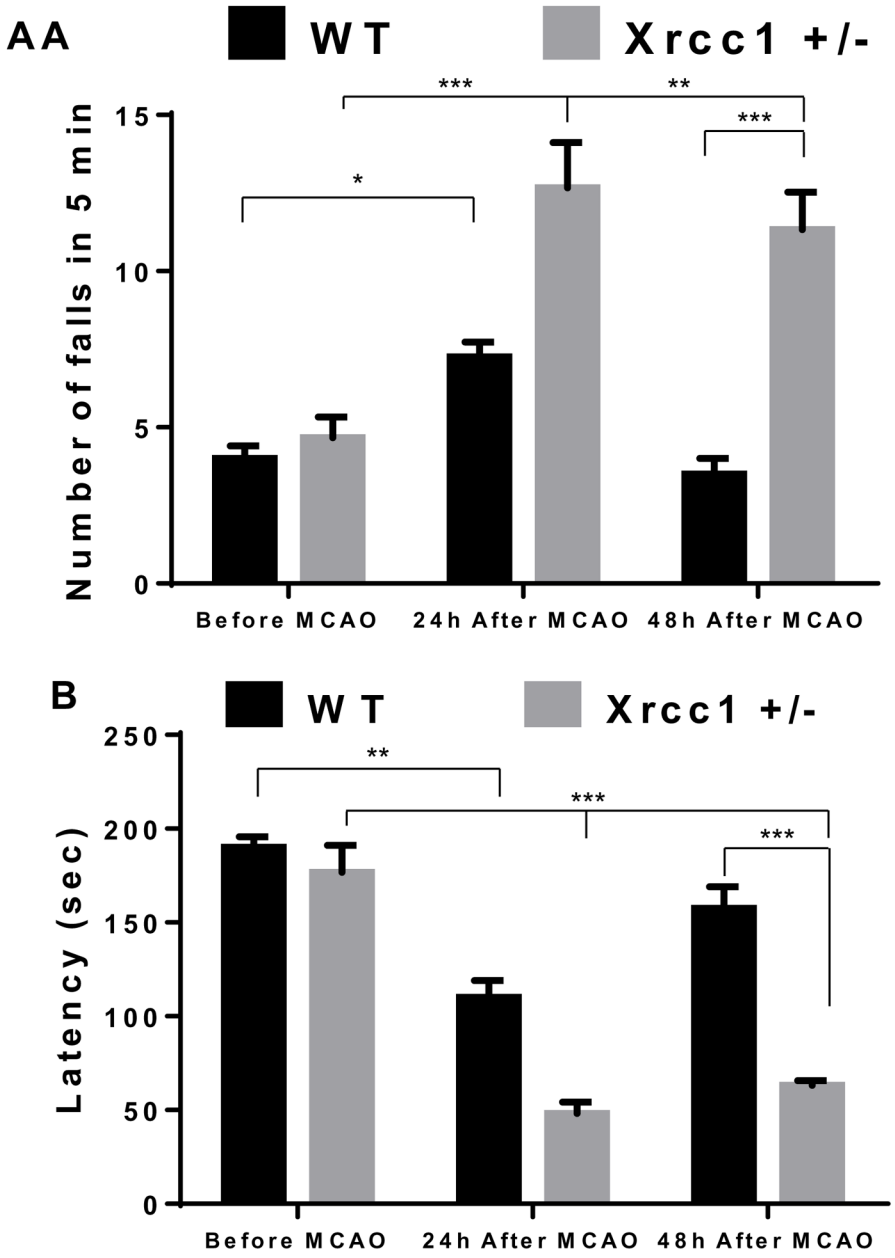

Figure 2.

Motor dysfunction in *Xrcc1* $^{+/-}$ and WT mice before and after middle cerebral artery occlusion/ reperfusion (MCAO/R). (A) Average number of falls and (B) average latency of first fall measured during rotarod test. Data indicate average ± SEM, where the sample size is WT, n = 4 and *Xrcc1* $^{+/-}$ n = 3. A two-way ANOVA followed by Bonferroni's correction as well as LSD was used to analyze the data. Asterisks denote the various p-values as follows: *, p≤0.024; **p≤0.001; *** p≤0.0001..

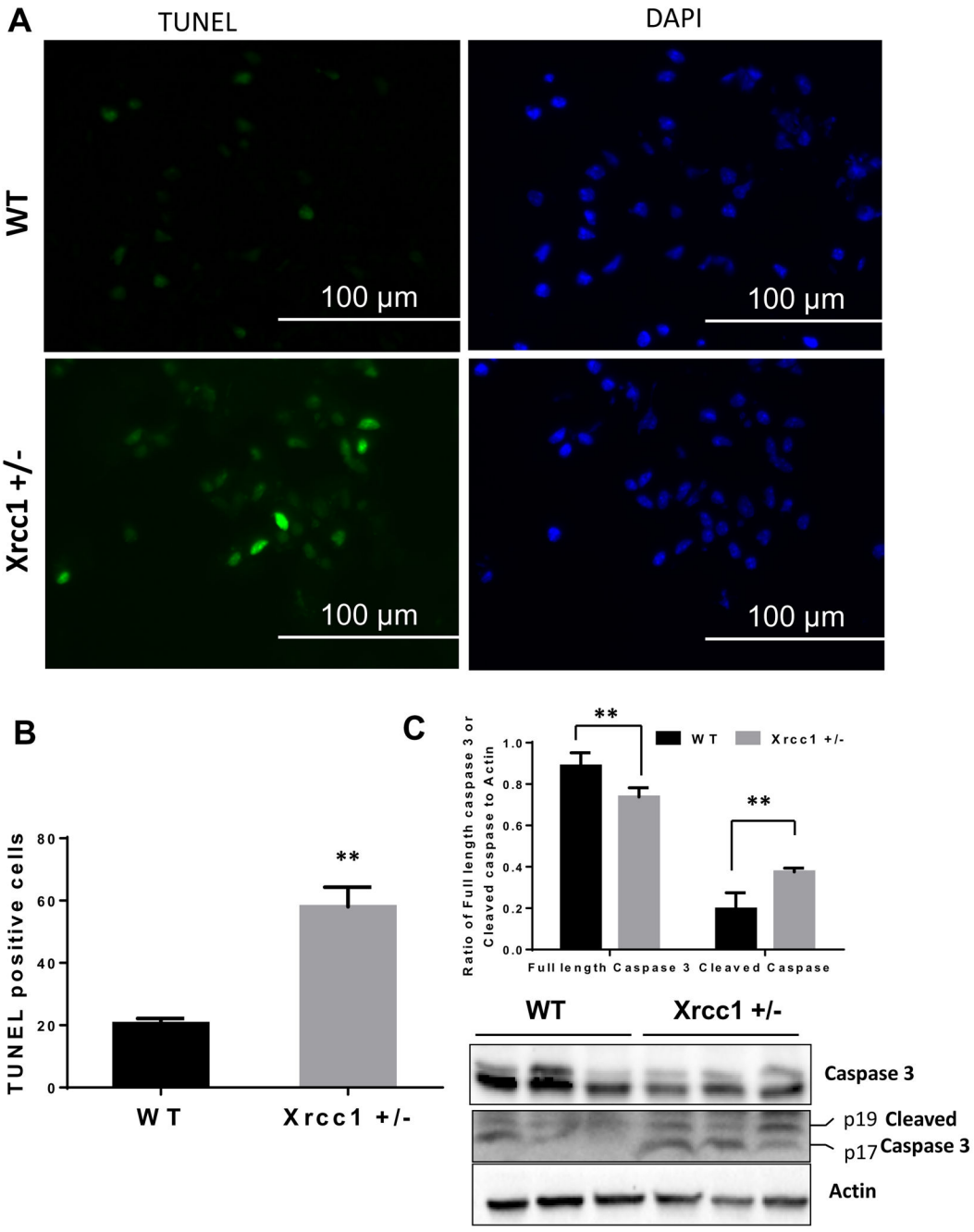

Figure 3.

Apoptosis in *Xrcc1* $^{+/-}$ mouse brains after middle cerebral artery occlusion/ reperfusion (MCAO/R). (A) Representative picture of a mouse brain section after TUNEL staining with FITC-labeled dUTP and terminal deoxynucleotidyl transferase enzyme in WT and *Xrcc1* $^{+/-}$ mouse brains after MCAO/R. (B) Quantification of TUNEL+ nuclei in WT and *Xrcc1* $^{+/-}$ mice. An average total TUNEL+ cells count was derived from at least six brain section areas using 4 WT and 3 *Xrcc1* $^{+/-}$ mice is shown. Data are mean ± SEM. *p<0.05, **p<0.01. Data were analyzed by two-tailed Student's *t*-test. (C) Levels of the full length and cleaved

caspase-3 in whole brain lysates of ipsilateral area of the stroked brains. The graph indicates the quantitation of full length caspase 3 and cleaved caspase 3 (sum of p19 + p17) levels shown in the blot normalized to the actin levels.

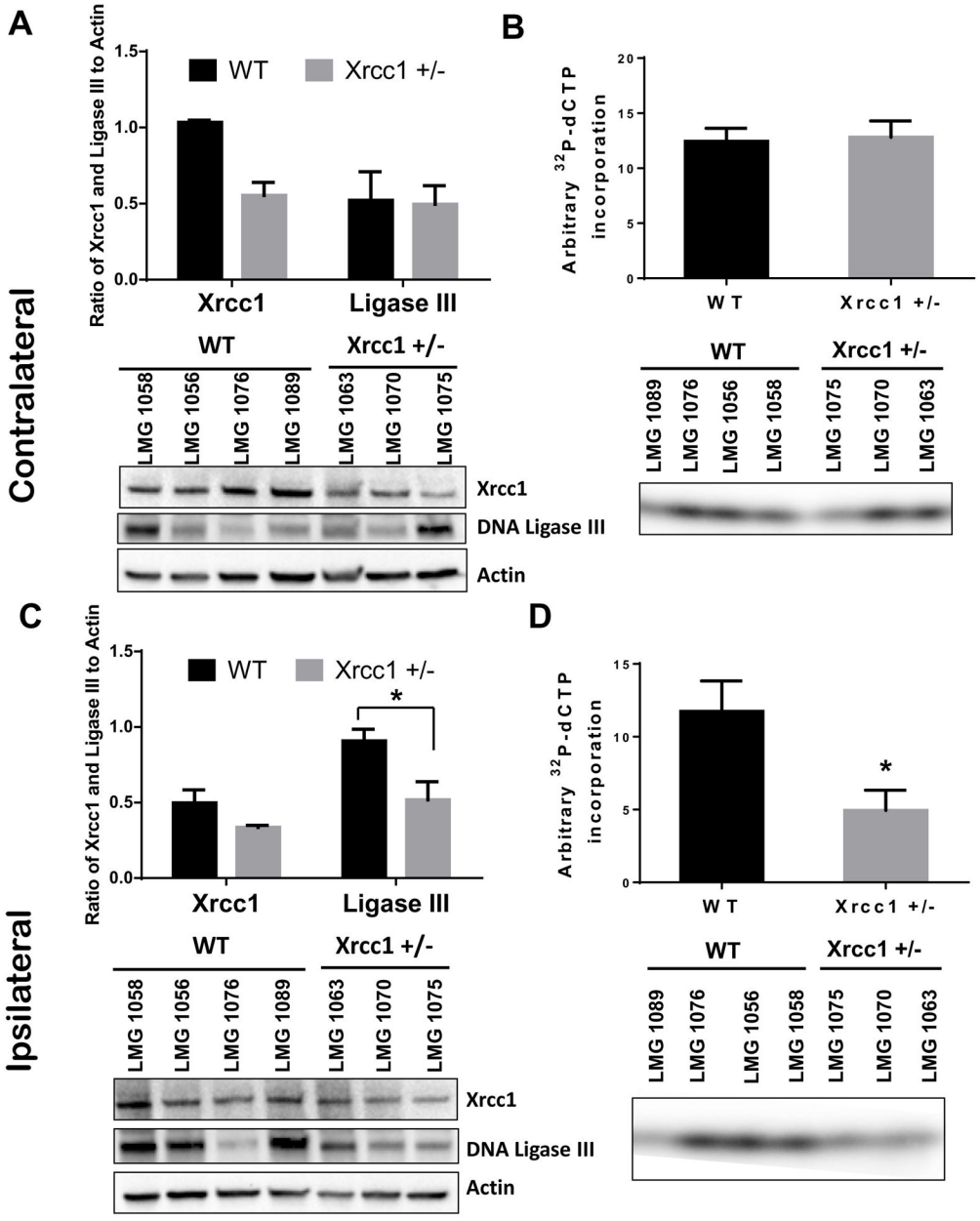

Figure 4.

Expression of Xrcc1 & DNA Ligase III and whole BER activity in *Xrcc1* $^{+/-}$ mouse brains after middle cerebral artery occlusion/ reperfusion (MCAO/R). (A) A representative immunoblot of Xrcc1 and Ligase III levels in whole brain lysates of contralateral area of the stroked brains. The graph indicates the quantitation of Xrcc1 and ligase III levels shown in the blot normalized to the actin levels. Data were averaged from 4 or 3 mice and at least two independent experiments. (B) Relative dCTP incorporation and ligation into a 91-mer in whole brain lysates of contralateral area of the stroked brains. Data indicate average ± SEM (*$p<0.05$ using a two-tailed Student's *t*-test with a sample size of n = 4 for WT and n = 3 for *Xrcc1* $^{+/-}$). (C) A representative immunoblot of Xrcc1 and Ligase III levels in whole brain lysates of ipsilateral area of the brains. The graph indicates the quantitation of Xrcc1 and

ligase III levels shown in the blot normalized to the actin levels. Data were represented from at least two experiments. (D) Relative dCTP incorporation and ligation into a 91-mer in whole brain lysates of ipsilateral area of the brains. Data indicate average ± SEM.

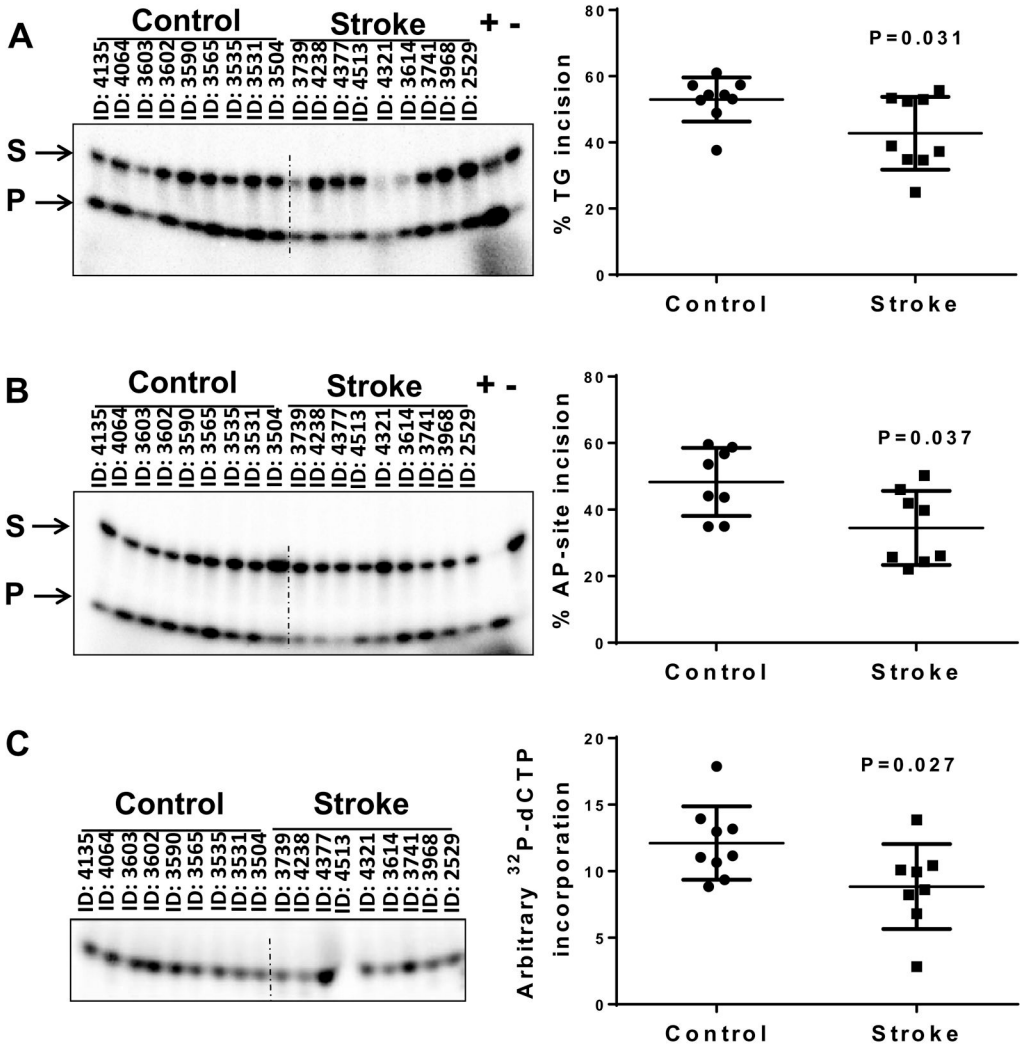

Figure 5.

BER activities in control and stroke human brain samples. (A) Whole tissue lysates from control and stroke postmortem brains were assessed for thymine glycol incision activity using oligonucleotide sequence (Table 2). (B) Whole tissue lysates from control and stroke postmortem brains were assessed for abasic site (tetrahydrofuran [THF]) cleavage using oligonucleotide sequence (Table 2). (C) Whole tissue lysates from control and stroke postmortem brains were assessed for deoxycytidinetriphosphate (dCTP) incorporation and ligation activity using oligonucleotide sequence (Table 2). The data are represented by mean ± SD, n = 9.

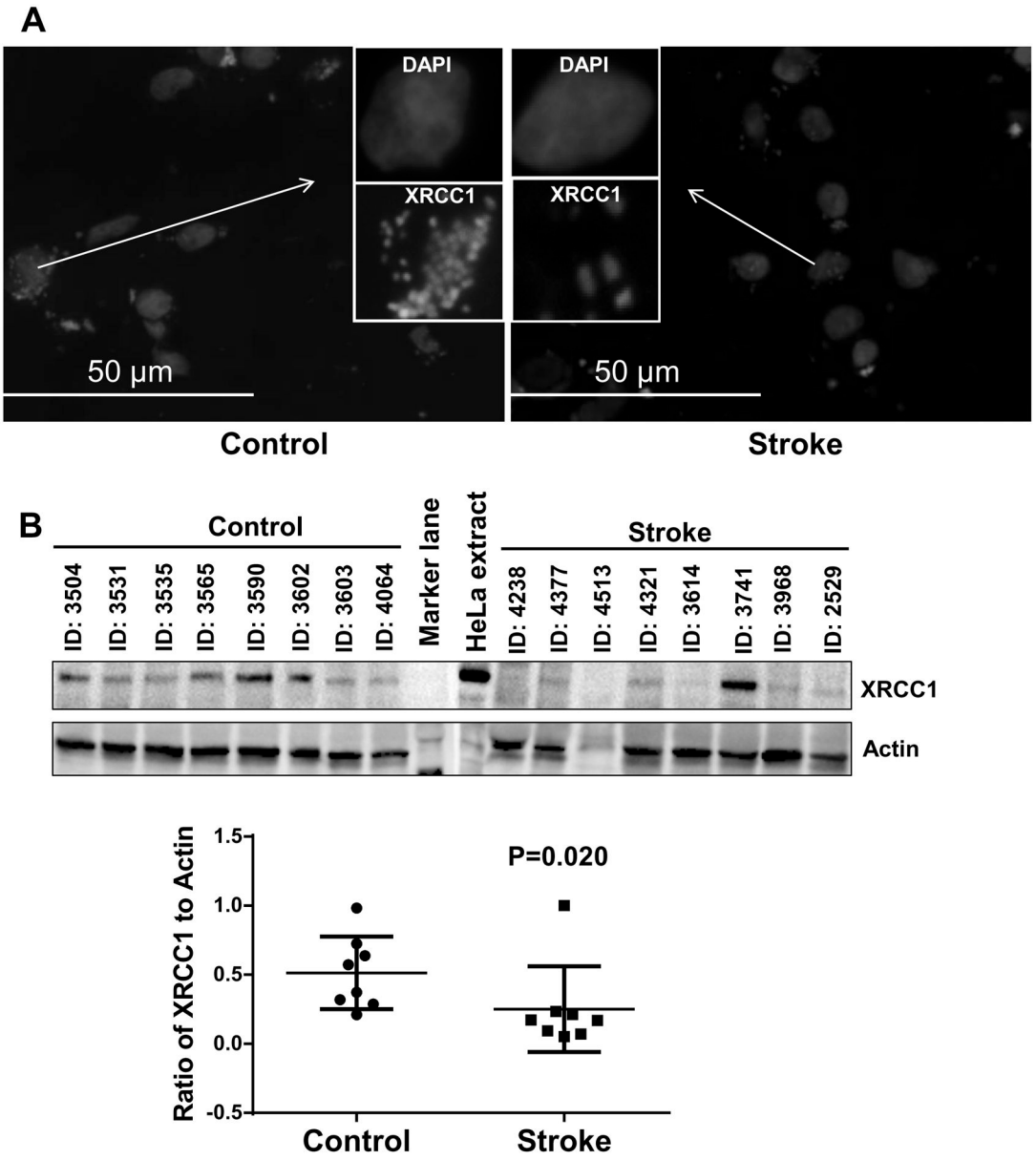

Figure 6.

XRCC1 expression in control and stroke human brain samples. (A) Representative image of Immunofluorescence staining of XRCC1 in control and stroke human brain samples, n=8 (Insert) image of a single cell is enlarged to show the expression of XRCC1. (B) A representative immunoblot of XRCC1 levels in control and stroke human brain samples. The graph indicates the quantitation of XRCC1 levels shown in the blot normalized to the actin levels. The data are represented by mean ± SD, n = 8.

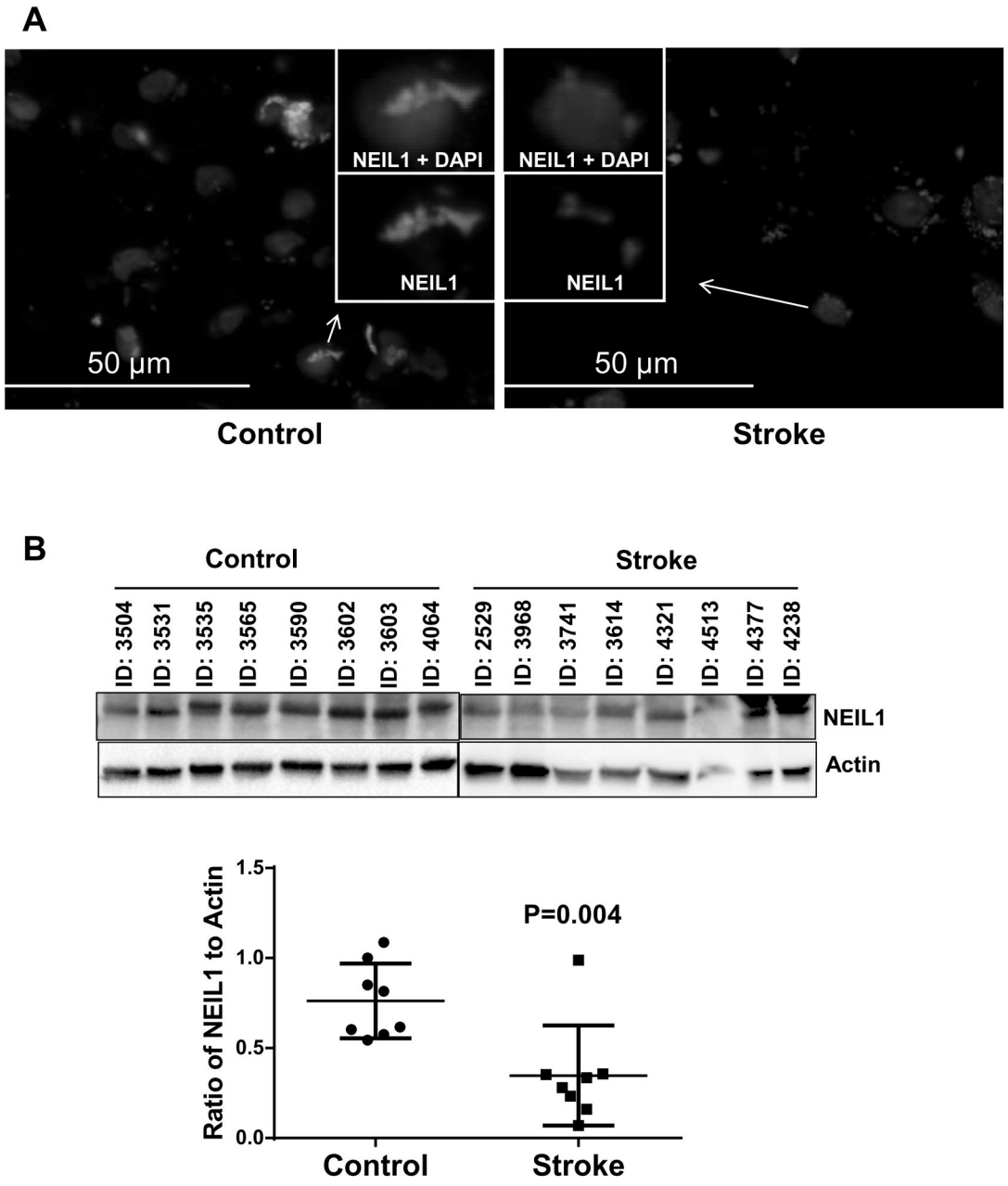

Figure 7.

NEIL1 expression in control and stroke human brain samples. (A) Representative image of Immunofluorescence staining of NEIL1 in control and stroke human brain samples, n=8 (Insert) image of a single cell is enlarged to show the expression of NEIL1. (B) A representative immunoblot of NEIL1 levels in control and stroke human brain samples. The graph indicates the quantitation of NEIL1 levels shown in the blot normalized to the actin levels. The data are represented by mean ± SD, n = 8.

Table 1

Details of tissue specimen obtained from the Human Brain and Spinal Fluid Resource Center, VA West Los Angeles Healthcare Center, Los Angeles, CA 90073 which is sponsored by NINDS/NIMH, National Multiple Sclerosis Society, and Department of Veterans Affairs.

Sample	PMI	Background	Age	Sex	Area	Cause of Death
2528	19.8	Stroke	76	F	Parietal Cortex	Stroke
3968	13.6	Stroke	81	F	Parietal Cortex	Stroke
3741	25.3	Stroke	76	F	Parietal Cortex	Stroke
3614	14.0	Stroke	84	M	Parietal Cortex	Stroke
4321	12.3	Stroke	85	M	Parietal Cortex	Stroke
4513	15.6	Stroke	74	M	Parietal Cortex	Stroke
4377	9.0	Stroke	87	F	Parietal Cortex	Stroke
4238	13.2	Stroke	84	M	Parietal Cortex	Stroke
3739	12.0	Stroke	62	F	Parietal Cortex	Stroke
3504	11.0	Non-neurological	80	M	Parietal Cortex	Renal Cancer
3531	13.6	Non-neurological	74	M	Parietal Cortex	Lung Cancer
3535	14.0	Non-neurological	81	M	Parietal Cortex	Non-Hodgkin Lymphoma
3565	11.0	Non-neurological	76	M	Parietal Cortex	Cardiomyopathy
3590	11.5	Non-neurological	75	M	Parietal Cortex	Coronary Heart Disease
3602	13.3	Non-neurological	66	M	Parietal Cortex	Bone and Liver metastasis
3603	12.0	Non-neurological	74	F	Parietal Cortex	Pancreas Cancer
4064	15.4	Non-neurological	75	F	Parietal Cortex	Liver Cancer
4135	12.6	Non-neurological	57	M	Parietal Cortex	Colon and Liver Cancer

Table 2

Names and sequences of oligonucleotides used in the study

Name	Sequence
TG-51mer	5’-TAATAATAACAATTGAATGTCT**(TG)**CACAGCCACTTTCCACACAGACATCAT-3’ 3’-ATTATTATTGTTAACTTACAGA**(A)**GTGTCGGTGAAAGGTGTGTCTGTAGTA-5’
THF-91mer	5’-TAATTAATGCTTGTAGGACATAATAATAACAATTGAATGTCT**(F)**CACA … 3’-ATTAATTACGAACATCCTGTATTATTATTGTTAACTTACAGA**(C)**GTGT … … GCCACTTTCCACACAGACATCATAACAAAAAATTTCCACCAAAC-3’ … CGGTGAAAGGTGTGTCTGTAGTATTGTTTTTTAAAGGTGGTTTG-5’
GAP-91mer	5’-TAATTAATGCTTGTAGGACATAATAATAACAATTGAATGTCT**G**CACA … 3’-ATTAATTACGAACATCCTGTATTATTATTGTTAACTTACAGA**( )**GTGT … … GCCACTTTCCACACAGACATCATAACAAAAAATTTCCACCAAAC-3’ … CGGTGAAAGGTGTGTCTGTAGTATTGTTTTTTAAAGGTGGTTTG-5’

TG containing thymine glycol; THF = containing a tetrahydrofuran abasic site analog; GAP =containing a single nucleotide gap.